RSC Advances

PAPER

View Article Online
View Journal | View Issue

Cite this: *RSC Adv.*, 2025, **15**, 15164

Novel C-3 and C-20 derived analogs of betulinic acid as potent cytotoxic agents: design, synthesis, *in vitro* and *in silico* studies†

Nisar A. Dangroo, *[a] Ziad Moussa, [b] Mustafa S. Alluhaibi,[c] Abdulrahman A. Alsimaree,[d] Mohammed B. Hawsawi, [c] Reem I. Alsantali,[e] Jasvinder Singh,[f] Nidhi Gupta, *[g] Basavarajaiah S. M., [h] Prashantha Karunakar,[i] J. M. Mir, [a] Manzoor A. Rather [a] and Saleh A. Ahmed *[cj]

In this report, novel derivatives of betulinic acid were designed and synthesized by targeting the C-3-OH group and C-20 olefinic bond in an endeavour to develop potent antitumor agents. These analogs were screened for their anticancer activity against six different human cancer cell lines including breast cancer MCF-7, lung cancer A549, colon cancer HCT-116, leukemia MOLT-4, prostate carcinoma cell PC-3 and pancreatic cancer cell Miapaca-2 by MTT assay. Many derivatives displayed better cytotoxicity than the parent compound BA. More significantly compounds **9b**, **9e**, **10** and **11a** were found to have more promising activity than BA. Compound **11a** was the most potent analog with IC_{50} values of 7.15 (MCF-7), 8.0 (A549), 3.13 (HCT-116), 13.88 (MOLT-4), 8.0 (PC-3) and 6.96 (MiaPaCa-2) μM. In addition to experimental investigations, *in silico* aspects were evaluated for the parent compound, BA and **11a** derivative based on its potential bioactive behaviour. The representative compounds were optimized structurally using density functional theory (DFT). GaussView 6.1 graphical interface associated GAUSSIAN 09 (Revision C.01) software package was used for the calculations under 6-311g(d,p)/B3LYP formalism using under a SMD model (water as solvent) for the parent compound BA and **11a** to explain the respective bioactive behaviour. This was followed by molecular docking studies suggesting that compound **11a** binds efficiently with all the three proteins with the docking score of −7.2 kcal mol^{-1} in the case of matrix metalloproteinase-2 (PDB ID: 1HOV) and poly[ADP-ribose] polymerase-1 (PDB ID: 1UK0) and −6.7 kcal mol^{-1} in the case of TRAF2 (PDB ID: 2X7F). Further, molecular dynamics studies between **11a** and the three proteins were carried out using Desmond Maestro v11.3 to study protein–ligand interactions and protein stability.

Received 12th February 2025
Accepted 29th April 2025

DOI: 10.1039/d5ra01038a

rsc.li/rsc-advances

Introduction

Cancer is a leading cause of death worldwide. According to a WHO report, in 2020, ten million deaths were contributed by cancer alone, and the most common cancers responsible for this mortality include lung, colon, liver, stomach and breast.[1] Colon cancer was found to be the third most common cancer worldwide and is the second leading cause of cancer related deaths. By the end of 2040, it is expected that the colon cancer burden will increase to 3.2 million new cancer cases and 1.6 million deaths each year.[2] Available treatments for colon cancer including surgery, chemotherapy, radiation and targeted therapy have certain limitations associated with them such as adverse side effects, multidrug resistance and limited

[a]*Department of Chemistry, Islamic University of Science and Technology, Awantipora, J & K, 192122, India. E-mail: nisar.iiim@gmail.com; nisar.ahmad@iust.ac.in*

[b]*Department of Chemistry, College of Science, United Arab Emirates University, P. O. Box 15551, Al Ain, United Arab Emirates*

[c]*Department of Chemistry, Faculty of Science, Umm Al-Qura University, 21955 Makkah, Saudi Arabia. E-mail: saahmed@uqu.edu.sa; saleh_63@hotmail.com*

[d]*Department of Chemistry, College of Science and Humanities, Shaqra University, Shaqra, Saudi Arabia*

[e]*Department of Pharmaceutical Chemistry, College of Pharmacy, Taif University, P. O. Box 11099, Taif 21944, Saudi Arabia*

[f]*The Hormel Institute, University of Minnesota, Austin, MN, USA*

[g]*MM College of Pharmacy, Maharishi Markandeshwar (Deemed to be University), Mullana-Ambala, Haryana 133207, India. E-mail: gupta21nidhi@gmail.com*

[h]*PG Department of Chemistry, Vijaya College, R. V. Road, Bengaluru 560 004, Karnataka, India*

[i]*Department of Biotechnology, Dayananda Sagar College of Engineering (Affiliated to Visvesvaraya Technological University, Belagavi), Kumaraswamy Layout, Bangalore 560111, Karnataka, India*

[j]*Department of Chemistry, Faculty of Science, Assiut University, 71516 Assiut, Egypt*

† Electronic supplementary information (ESI) available. See DOI: https://doi.org/10.1039/d5ra01038a

availability. There is an urgent need for the development of novel anti-colon cancer agents with fewer side effects and greater efficacy.[3] Natural products have played a highly significant role as a source of lead molecules for anticancer drug discovery. In the timeframe of 39 years, from 1981 to 2019, out of 185 small molecules as anticancer drugs, 75 were related to natural products and their derivatives.[4] Among the natural products, triterpenoids of lupane-, oleanane-, ursane- and cucurbitane-type and their structural derivatives have been reported for their potent *in vitro* and *in vivo* anticancer effects.[5]

Betulinic acid (BA), a pentacyclic lupane-type triterpenoid, exhibits anticancer effects with various mode of action including triggering the apoptosis in cancer cells *via* activating mitochondrial pathway, regulating the cell cycle and angiogenesis *via* different factors such as specificity protein transcription factors, cyclin D1 and epidermal growth factor receptor, inhibition of signal transducer and activator of transcription 3 and NFκB signalling pathways. It also prevents the invasion and metastasis of tumor cells, and affects the topoisomerase I, p53 and lamin B1 expression.[6] BA is a pharmacologically active scaffold but possess low water solubility, poor bioavailability and less efficacy.[7] As such a number of analogs have been reported by exploiting the key positions C-2, C-3, C-20 and C-28 available on the BA (Fig. 1). Several BA modified derivatives having polar sugar moiety at C-3 (**2**, **3**) and 3,4-*seco* (**4**) derivatives have been reported in literature for improved water solubility as well as promising cytotoxicity against cancer cell lines.[8] Miao *et al.* reported the betulinic acid carbamate derivative **5** at C-3 as human CD73 inhibitor and promising immuno-oncology target.[9] NVX-207, a C-28 modified BA derivative reported to possess cytotoxicity on several cancer cell lines. Paschke *et al.* reported the anticancer effects of BA and its two C-3 modified derivatives (**6** & **7**) including NVX-207 for antiproliferative effects on equine and human melanoma cell lines. NVX-207 beside having the improved water solubility was found to be the potent antiproliferative agent among all three compounds.[10] Some selected C-3 modified derivatives of betulinic acid are shown in Fig. 1.

In continuation to our previous communications,[11–13] in the present paper, we report the synthesis of new analogs by targeting less explored C-3 and C-20 positions of BA. The new derivatives were evaluated against six different human cancer cell lines including MCF-7, A549, HCT-116, MOLT-4, PC-3 and Miapaca-2. In addition to experimental studies, DFT calculations were done using reliable level of theory to speculate optimized structure and various other physicochemical properties. Molecular docking studies were carried out against three targets involved in pathophysiology of colon cancer including matrix metalloproteinase-2 (PDB ID: 1HOV), poly[ADP-ribose] polymerase-1 (PDB ID: 1UK0) and TRAF2 (PDB ID: 2X7F). The molecular dynamics simulation studies of lead compound and above-mentioned proteins were evaluated to determine ligand protein interactions and stability.

Material and methods

All the chemicals and reagents for synthesis were purchased from Sigma Aldrich. The chemical reactions monitored using

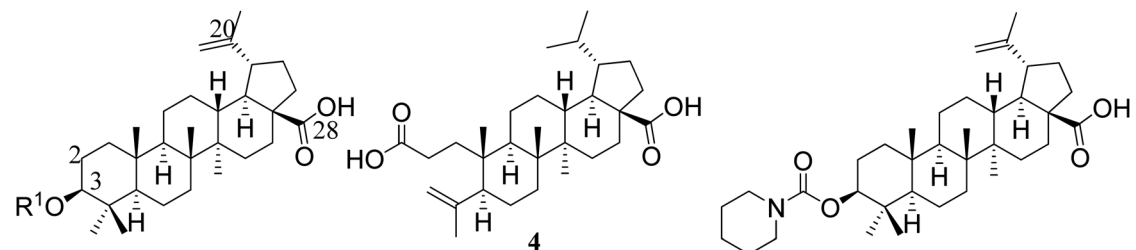

R^1	A549 IC_{50} (μM/L)
1 H	10.3
2 Rha	2.6
3 Ara	10

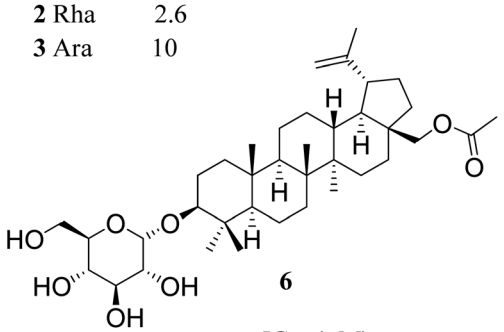

	IC_{50} (μM)
A375	10.3
MelDuWi	11.6
MelJess	11.8

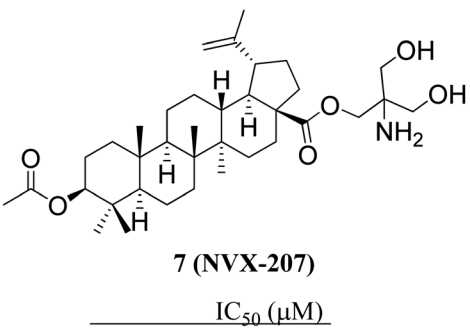

	IC_{50} (μM)
A375	2.6
MelDuWi	5.6
MelJess	6.5

Fig. 1 Some selected C-3 modified betulinic acid derivatives (2–7) as anticancer agents.

silica gel F_{254} plates using ceric ammonium sulphate solution as spraying reagent for detection of spots. The synthesized products were purified *via* column chromatography using silica gel 60–120 mesh as stationary phase. NMR spectra of all the compounds recorded on Bruker DPX 400 and DPX 500 instrument using $CDCl_3$ solvent. The chemical shifts are expressed in δ and coupling constant in Hertz. High Resolution Mass Spectra (HRMS) were recorded on Agilent Technologies 6540 instrument.

Isolation of betulinic acid (1)

Betulinic acid (**1**) was isolated from the stem bark of *Platanus orientalis*. Shade dried and course powdered plant material (1.6 kg) was extracted with DCM–methanol (1 : 1) at room temperature for 24 h, and filtered. The marc was re-extracted twice with same solvent proportions. The filtrate was concentrated on rotary evaporator at 40 °C under reduced pressure and afforded about 120 grams of DCM–methanol extract (extractive value (EV) = 7.5%). The desired compound was purified by column chromatography over silica gel 60–120 mesh and further purified by repeated crystallization. The NP was characterized using various spectroscopic techniques and comparison of data with that reported in the literature.[12]

Preparation of 3-chloroacetyl betulinic acid (8)

To compound **1** (1.0 g, 2.2 mmol) dissolved in dry THF (20 mL) was added pyridine (3.3 mmol) and stirred at 0 °C for 5–10 minutes. Chloroacetyl chloride (0.31 mL, 4.4 mmol) was then added dropwise while stirring at 0 °C. After addition, the reaction mixture was allowed to react at room temperature till completion for 2–3 h monitored by TLC. To the reaction mixture was then added 50 mL of ice-cold water and allow the crude product to precipitate and then recrystallized in methanol and DCM furnished **2** as white solid (96% yield). ^{1}H NMR ($CDCl_3$, 400 MHz): δ 4.71 and 4.61 (1H, each, s, H-29), 4.56 (1H, t, J = 8.8 Hz, H-3), 4.05 (2H, d, J = 1.9 Hz, COCH_2Cl), 3.00 (1H, m, H-19), 2.26 and 1.66 (1H, each, m, H-22), 2.19 and 1.51 (1H each, m, H-16), 1.97 (2H, m, H-2), 1.69 (3H, s, H-30), 1.66 (1H, m, H-13), 1.62 (1H, m, H-18), 1.63 and 1.39 (1H each, m, H-6), 1.52 and 1.25 (1H each, m, H-15), 1.55 and 1.41 (1H each, m, H-7), 1.42 and 1.17 (1H each, m, H-21), 1.38 and 1.25 (1H each, m, H-12),1.38 (1H, m, H-9), 1.06 and 1.16 (1H each, m, H-11), 1.61 and 1.10 (1H each, m, H-1), 0.97 (3H, s, H-26), 0.93 and 0.86 (3H, each, s, H-27 and H-23), 0.85 (3H, s, H-24), 0.85(3H, s, H-25), 0.80 (1H, m, H-5); ^{13}C NMR (125 MHz, $CDCl_3$) δ 182.92, 167.21, 150.37, 109.80, 83.38, 56.43, 55.34, 50.34, 49.22, 46.96, 42.42, 41.29, 40.66, 38.40, 38.27, 38.02, 38.01, 37.09, 34.1, 32.14, 30.56, 29.68, 27.94, 25.39, 23.55, 20.85, 19.36, 18.11, 16.42, 16.17, 16.03, 14.67. HRMS m/z calcd for $C_{32}H_{49}ClO_4$ $[M + H]^+$ 533.0230, found 533.0236.

General procedure for the preparation of amino derivatives (9a–g)

The title compounds **9a–g** were prepared by dissolving compound **8** (0.2 mmol) in THF and was added appropriate amine (0.3 mmol) and pyridine (0.2 mmol) and stirred at room temperature. Upon completion of the reaction as monitored by TLC, the reaction mixture was poured onto 50 mL of water and partitioned with ethyl acetate (3 × 20 mL). The organic layer was dried over Na_2SO_4 and purified *via* silica gel column chromatography/by recrystallization to afford the desired products in excellent yields. The spectral data of the compounds is given in the ESI.†

Preparation of 3-azidoacetyl betulinic acid (10)

The title compound was synthesised by reaction of **8** (0.2 mmol) with NaN_3 (0.4 mmol) in THF : water (2 : 1) at room temperature. After completion of the reaction, the reaction mixture was poured in ice cold water to allow the crude product to precipitate. The precipitate was finally washed with methanol to furnish 10 (yield 85%).^{1}H NMR ($CDCl_3$, 400 MHz): δ 4.74 and 4.62 (1H, each, s, H-29), 4.57 (1H, m, H-3), 3.49 (2H, s, COCH_2N$_3$), 3.00 (1H, m, H-19), 2.27 and 1.66 (1H, each, m, H-22), 2.19 and 1.51 (1H each, m, H-16), 1.97 (2H, m, H-2), 1.69 (3H, s, H-30), 1.66 (1H, m, H-13), 1.62 (1H, m, H-18), 1.63 and 1.39 (1H each, m, H-6), 1.52 and 1.25 (1H each, m, H-15), 1.55 and 1.41 (1H each, m, H-7), 1.42 and 1.17 (1H each, m, H-21), 1.38 and 1.25 (1H each, m, H-12),1.38 (1H, m, H-9), 1.06 and 1.16 (1H each, m, H-11), 1.61 and 1.10 (1H each, m, H-1), 0.97 (3H, s, H-26), 0.93 and 0.85(3H, each, s, H-27 and H-23), 0.87 (3H, s, H-24), 0.85 (3H, s, H-25), 0.79 (1H, m, H-5). HRMS m/z calcd for $C_{32}H_{49}N_3O_4$ $[M + H]^+$ 540.0124, found 540.0125.

Synthesis of phosphoramidate 11a

The compound **10** (0.2 mmol) dissolved in THF and to this added trimethylphosphite (0.3 mmol), and the reaction was stirred at room temperature till completion. The reaction mixture was poured onto 30 mL of water and partitioned with ethyl acetate (3 × 20 mL). The organic layer was dried over Na_2SO_4 and purified *via* silica gel column chromatography in 5% methanol/dichloromethane as eluent to afford the desired product **5a** in 58% yield.^{1}H NMR ($CDCl_3$, 400 MHz): δ 4.72 and 4.59 (1H, each, s, H-29), 4.53 (1H, t, J = 8.0 Hz, H-3), 3.73 and 3.70 (6H, each, s, 2× OCH_3), 3.67 (2H, m, COCH_2NH), 3.25 (1H, m, NH), 2.98 (1H, m, H-19), 2.26 and 1.65 (1H, each, m, H-22), 2.18 and 1.47 (1H each, m, H-16), 1.95 (2H, m, H-2), 1.68(3H, s, H-30), 1.64 (1H, m, H-13), 1.61 (1H, m, H-18), 1.59 and 1.39 (1H each, m, H-6), 1.52 and 1.25 (1H each, m, H-15), 1.54 and 1.41 (1H each, m, H-7), 1.41 and 1.17 (1H each, m, H-21), 1.37 and 1.23 (1H each, m, H-12),1.34(1H, m, H-9), 1.15 and 1.07 (1H each, m, H-11), 1.62 and 1.02 (1H each, m, H-1), 0.95 (3H, s, H-26), 0.91 (3H, s, H-24), 0.82 (6H, each, s, H-27 and H-23), 0.80(3H, s, H-25), 0.76 (1H, m, H-5). ^{13}C NMR (125 MHz, $CDCl_3$) δ 181.39, 170.64, 150.55, 109.65, 82.57, 56.32, 55.39, 53.33, 53.32, 50.39, 49.20, 46.91, 42.97, 42.42, 40.68, 38.31, 37.91, 37.09, 34.19, 32.20, 30.58, 29.68, 27.95, 25.42, 23.68, 20.86, 19.36, 18.13, 16.45, 16.18, 15.98, 14.65, 14.14. HRMS m/z calcd for $C_{34}H_{56}NO_7P$ $[M + H]^+$ 622.2654, found 622.2656.

Synthesis of phosphoramidate 11b

The compound **10** (0.2 mmol) dissolved in THF was added triethylphosphite (0.3 mmol). The reaction mixture was stirred at room temperature till completion. The reaction mixture was poured onto 30 mL of water and partitioned with DCM (3 × 20 mL). The organic layer was dried over Na_2SO_4 and purified *via* silica gel column chromatography in 5% methanol dichloromethane as eluent to afford the desired product **11b** in 60% yield. ^{1}H NMR ($CDCl_3$, 400 MHz): δ 4.72 and 4.60 (1H, each, s, H-29), 4.56 (1H, t, J = 8.4 Hz, H-3), 3.68 (2H, m, COC*H*$_2$NH), 3.70 (4H, m, 2× OC*H*$_2$CH$_3$), 3.39 (1H, m, N*H*), 3.00 (1H, m, H-19), 2.24 and 1.63 (1H, each, m, H-22), 2.17 and 1.48 (1H each, m, H-16), 1.97 (2H, m, H-2), 1.68 (3H, s, H-30), 1.65 (1H, m, H-13), 1.62 (1H, m, H-18), 1.63 and 1.39 (1H each, m, H-6), 1.52 and 1.25 (1H each, m, H-15), 1.55 and 1.41 (1H each, m, H-7), 1.42 and 1.17 (1H each, m, H-21), 1.37 and 1.23 (1H each, m, H-12),1.35 (1H, m, H-9), 1.15 and 1.07 (1H each, m, H-11), 1.61 and 1.10 (1H each, m, H-1), 1.31 (6H, m, 2× CH$_2$C*H*$_3$), 0.96 (3H, s, H-26), 0.92 (3H, s, H-24), 0.83 (6H, each, s, H-27 and H-23), 0.81(3H, s, H-25), 0.78 (1H, m, H-5). ^{13}C NMR (125 MHz, $CDCl_3$) δ 181.33, 170.66, 150.55, 109.65, 82.53, 62.67, 62.79, 56.32, 55.39, 53.32, 53.18, 53.29, 50.39, 49.21, 46.91, 43.00, 42.42, 40.68, 38.30, 37.91, 37.09, 34.20, 32.20, 30.59, 29.68, 27.96, 25.43, 23.69, 20.87, 19.36, 18.14,16.45, 16.18, 16.13, 15.99, 14.65. HRMS *m*/*z* calcd for $C_{36}H_{60}NO_7P$ $[M + H]^+$ 650.2005, found 650.2007.

Synthesis of compound 12

To a solution of compound **1** (1.0 mmol) in dry THF taken in an oven dried and air tight RB was added *N*-bromosuccinimide (1.25 mmol). The heterogeneous reaction mixture was stirred at room temperature till completion monitored by TLC. The reaction mixture was poured onto 100 mL of water and partitioned with DCM (3 × 50 mL). The organic layer was dried over Na_2SO_4 and purified *via* silica gel column chromatography in 12% ethyl acetate/hexane as eluent to afford the desired product **12** in 76% yield. ^{1}H NMR ($CDCl_3$, 400 MHz): δ 5.14 and 5.05 (1H, each, s, H-29), 4.0 (2H, s, H-23), 3.15 (1H, t, J = 7.6 Hz, H-3), 3.05 (1H, ddd, J = 4.8, 4.3, 4.4 Hz, H-19), 2.29 and 1.67 (1H, each, m, H-22), 2.26 and 1.47 (1H each, m, H-16), 1.93 (2H, m, H-2), 1.73 (3H, s, H-30), 1.69 (1H, m, H-13), 1.67 (1H, m, H-18), 1.63 and 1.42 (1H each, m, H-6), 1.58 and 1.37 (1H each, m, H-15), 1.56 and 1.42 (1H each, m, H-7), 1.41 and 1.17 (1H each, m, H-21), 1.38 and 1.23 (1H each, m, H-12),1.35 (1H, m, H-9), 1.15 and 1.07 (1H each, m, H-11), 1.62 and 1.02 (1H each, m, H-1), 0.96 (3H, s, H-26), 0.95 (3H, s, H-24), 0.82 (3H, each, s, H-27), 0.75 (3H, s, H-25), 0.68 (1H, m, H-5); ^{13}C NMR (125 MHz, $CDCl_3$) δ 178.87, 151.49, 146.08, 113.14, 101.07, 78.62, 56.20, 55.33, 50.68, 50.47, 47.63, 42.23 40.58, 38.75, 38.24, 37.08, 36.77, 34.30, 33.05, 32.08, 31.22, 30.01, 27.74, 26.80, 20.94, 18.22, 15.98, 15.77, 15.25, 14.53. HRMS *m*/*z* calcd for $C_{30}H_{47}BrO_3$ $[M + H]^+$ 535.2300, found 535.2301.

Synthesis of compound 7

To a solution of compound **13** (0.6 mmol) in THF : water (1 : 1) was added NaN_3 (0.9 mmol) and stirred at room temperature till completion of the reaction. The reaction mixture was poured onto 50 mL of water and partitioned with DCM (3 × 30 mL). The organic layer was dried over Na_2SO_4 and purified *via* silica gel column chromatography in 15% ethyl acetate hexane as eluent to afford the desired product **13** in 70% yield. ^{1}H NMR ($CDCl_3$, 400 MHz): δ 5.04 and 4.96 (1H, each, s, H-29), 3.76 (2H, s, H-23), 3.19 (1H, dd, J = 5.2, 4.8 Hz, H-3), 2.95 (1H, ddd, J = 4.4, 4.3, 4.4 Hz, H-19), 2.29 and 1.67 (1H, each, m, H-22), 2.27 and 1.47 (1H each, m, H-16), 1.93 (2H, m, H-2), 1.73 (3H, s, H-30), 1.69 (1H, m, H-13), 1.67 (1H, m, H-18), 1.63 and 1.42 (1H each, m, H-6), 1.58 and 1.37 (1H each, m, H-15), 1.56 and 1.42 (1H each, m, H-7), 1.41 and 1.17 (1H each, m, H-21), 1.38 and 1.23 (1H each, m, H-12),1.35 (1H, m, H-9), 1.19 and 1.07 (1H each, m, H-11), 1.62 and 0.95 (1H each, m, H-1), 0.96 (3H, s, H-26), 0.93 (3H, s, H-24), 0.82 (3H, each, s, H-27), 0.75 (3H, s, H-25), 0.69 (1H, m, H-5). ^{13}C NMR (125 MHz, $CDCl_3$) ^{13}C NMR (126 MHz, $CDCl_3$) δ 178.83, 149.09, 111.21, 78.76, 56.16, 55.40, 55.29, 50.44, 50.22, 48.85, 43.52, 42.32, 40.63, 38.73, 38.15, 37.09, 36.77, 34.28, 32.05, 31.89, 29.58, 27.80, 26.93, 26.78, 20.93, 18.20, 16.00, 15.81, 15.25, 14.54. HRMS *m*/*z* calcd for $C_{30}H_{47}N_3O_3$ $[M + H]^+$ 498.0125, found 498.0129.

Synthesis of compound 14a

The compound **13** (0.2 mmol) dissolved in THF and was added trimethylphosphite (0.3 mmol) and stirred at room temperature till completion. The reaction mixture was poured onto 30 mL of water and partitioned with DCM (3 × 20 mL). The organic layer was dried over Na_2SO_4 and purified *via* silica gel column chromatography in 5% methanol/dichloromethane as eluent to afford the desired product **14a** in 61% yield.^{1}H NMR ($CDCl_3$, 400 MHz): δ 4.98 and 4.89 (1H, each, s, H-29), 4.07 (4H, m, OC*H*$_2$CH$_3$), 3.45 (3H, m, H-23, *NH*), 3.19 (1H, dd, J = 5.2, 4.8 Hz, H-3), 2.88 (1H, ddd, J = 4.4, 4.3, 4.4 Hz, H-19), 2.28 and 1.67 (1H, each, m, H-22), 2.27 and 1.47 (1H each, m, H-16), 1.93 (2H, m, H-2), 1.73 (3H, s, H-30), 1.69 (1H, m, H-13), 1.67 (1H, m, H-18), 1.63 and 1.42 (1H each, m, H-6), 1.58 and 1.37 (1H each, m, H-15), 1.56 and 1.42 (1H each, m, H-7), 1.41 and 1.17 (1H each, m, H-21), 1.38 and 1.23 (1H each, m, H-12),1.35 (1H, m, H-9), 1.31 (6H, m, OCH$_2$C*H*$_3$), 1.19 and 1.07 (1H each, m, H-11), 1.62 and 0.95 (1H each, m, H-1), 0.96 (3H, s, H-26), 0.91 (3H, s, H-24), 0.81 (3H, each, s, H-27), 0.75 (3H, s, H-25), 0.67 (1H, m, H-5). ^{13}C NMR (125 MHz, $CDCl_3$) δ 180.39, 153.01, 106.98, 78.93, 62.31 (2× *C*H$_2$), 56.20, 55.30, 50.44, 50.14, 45.21, 43.25, 42.34, 40.66, 38.85, 38.67, 38.22, 37.16, 36.82, 34.30, 32.35, 31.95, 29.39, 28.01, 27.26, 26.81, 22.72, 21.00, 18.28, 16.23, 16.18, 16.02, 15.43, 14.70, 14.17. HRMS *m*/*z* calcd for $C_{32}H_{54}NO_6P$ $[M + H]^+$ 580.0417, found 580.0419.

Synthesis of compound 14b

To a solution of compound **13** (0.2 mmol) in THF and was added triethylphosphite (0.3 mmol) and stirred at room temperature. After completion, the reaction mixture was poured onto 30 mL of water and partitioned with DCM (3 × 20 mL). The organic layer was dried over Na_2SO_4 and purified *via* silica gel column chromatography in 5% methanol/dichloromethane as eluent to afford the desired product **14b** in 68% yield. ^{1}H NMR ($CDCl_3$, 400 MHz): δ 4.98 and 4.89 (1H, each, s, H-29), 4.07 (4H, m,

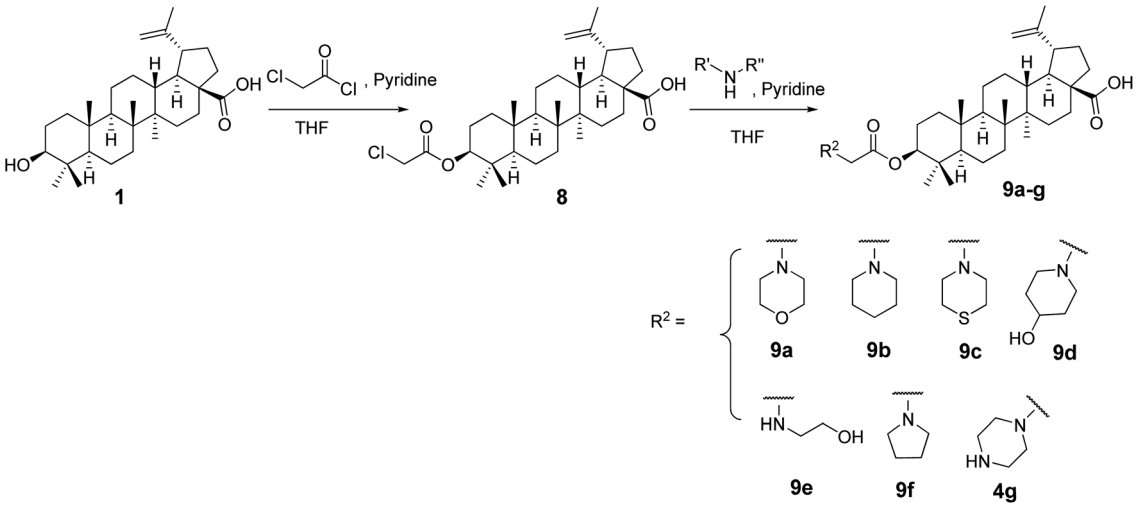

Scheme 1 Synthetic route to **9a–g**.

OCH_2CH_3), 3.45 (3H, m, H-23, N*H*), 3.19 (1H, dd, $J = 5.2$, 4.8 Hz, H-3), 2.88 (1H, ddd, $J = 4.4$, 4.3, 4.4 Hz, H-19), 2.28 and 1.67 (1H, each, m, H-22), 2.27 and 1.47 (1H each, m, H-16), 1.93 (2H, m, H-2), 1.73 (3H, s, H-30), 1.69 (1H, m, H-13), 1.67 (1H, m, H-18), 1.63 and 1.42 (1H each, m, H-6), 1.58 and 1.37 (1H each, m, H-15), 1.56 and 1.42 (1H each, m, H-7), 1.41 and 1.17 (1H each, m, H-21), 1.38 and 1.23 (1H each, m, H-12),1.35 (1H, m, H-9), 1.31 (6H, m, OCH_2CH_3), 1.19 and 1.07 (1H each, m, H-11), 1.62 and 0.95 (1H each, m, H-1), 0.96 (3H, s, H-26), 0.91 (3H, s, H-24), 0.81 (3H, each, s, H-27), 0.75 (3H, s, H-25), 0.67 (1H, m, H-5). ^{13}C NMR (125 MHz, $CDCl_3$) δ 180.39, 153.01, 106.98, 78.93, 62.31 (2× CH_2), 56.20, 55.30, 50.44, 50.14, 45.21, 43.25, 42.34, 40.66, 38.85, 38.67, 38.22, 37.16, 36.82, 34.30, 32.35, 31.95, 29.39, 28.01, 27.26, 26.81, 22.72, 21.00, 18.28, 16.23, 16.18, 16.02, 15.43, 14.70, 14.17. HRMS *m*/*z* calcd for $C_{34}H_{58}NO_6P$ $[M + H]^+$ 608.2145, found 608.2147.

Biological assay

Cell culture and treatment. The human cancer cell lines including breast cancer cell MCF-7, lung cancer A549, colon cancer HCT-116, leukemia MOLT-4, prostate carcinoma PC-3 and pancreatic cancer Miapaca-2 were purchased from ECACC, England. Cancer cells were grown in RPMI/MEM/McCOY/DMEM growth media containing 10% FCS, 100 U

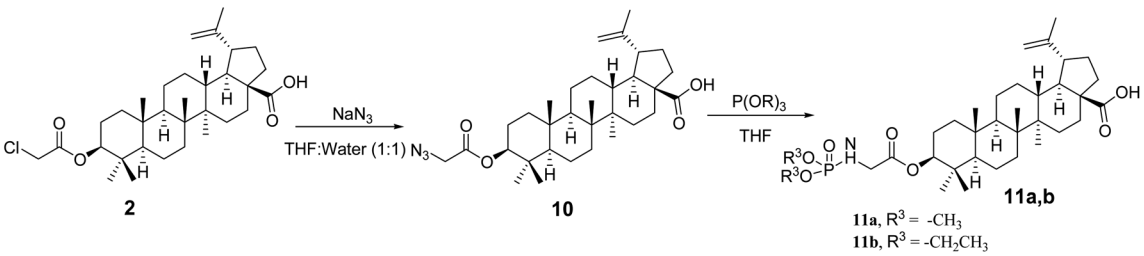

Scheme 2 Synthetic route to **10**, **11a** and **11b**.

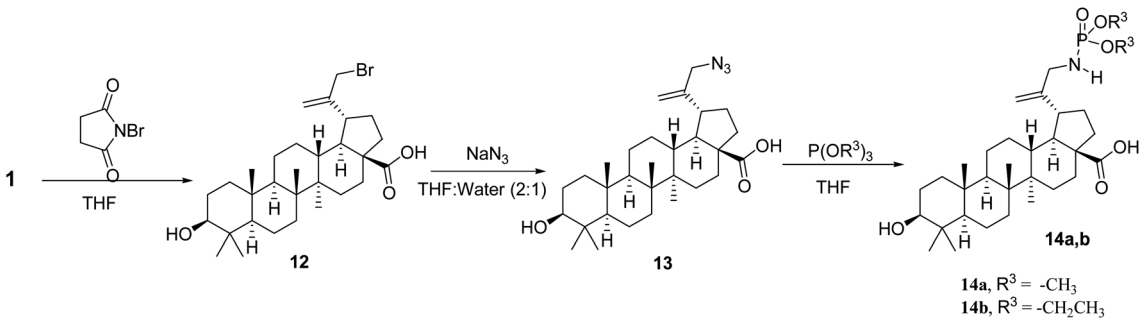

Scheme 3 Synthetic route to **14a** and **14b**.

penicillin G, and 100 μg streptomycin per mL. Cells were grown in a CO_2 incubator (Thermocon Electron Corporation, Texas, USA) at 37 °C with 95% humidity. Cells were treated with compounds dissolved in DMSO while the untreated control cultures received only DMSO with concentration <0.2%.

Cell proliferation assay. Cells were seeded in 96 well plates. When at 70–75% confluency after 4 h, cells were treated with given compounds and placed in incubator for 48 h. MTT dye was added to the plates 4 h prior to experiment termination at concentration of 2.5 mg mL^{-1}, dissolved in media. MTT formazon crystals formed were dissolved in DMSO and absorbance at 570 nm was recorded.[12]

DFT evaluation. The energy minimal state or optimized structural conformation of the target compounds, was obtained by optimizing at the DFT level 6-311g(d,p) basis set along with B3LYP functional. GaussView 6.1 graphical interface associated GAUSSIAN 09 (Revision C.01) was the software-package used for the different calculations and visualization of results. BA and **11a** in their carboxylate forms have been computed and compared to explain the bioactive behaviour. Various systematic algorithms under combined non-planar group symmetry and theoretical force constants generate useful conclusions from the calculation. Molecular orbital analysis, and other electron density mapping[14] were further analysed to describe various physicochemical properties linked with the study.[15,16]

Molecular docking and dynamic studies

Protein preparation. The 3-dimensional structures of proteins were retrieved from RCSB PDB (Research Collaboratory for Structural Bioinformatics PDB). Matrix metalloproteinase-2 bound to *N*-[4-[[(2*R*)-1-(hydroxyamino)-3-methyl-1-oxo-butan-2-yl]-(2-morpholin-4-ylethyl)sulfamoyl]phenyl]-4-pentyl-benzamide (ligand id: SC-74020 or I52) (PDB id: 1HOV), structure of catalytic domain of human poly(ADP-ribose) polymerase in complex with 2-[3-[(1*R*)-4-(4-fluorophenyl)-3,6-dihydro-2*H*-pyridin-1-yl]propyl]-8-methyl-3*H*-quinazolin-4-one (ligand id: FRM) (PDB id: 1UK0) and structure of the Kinase Domain of Human Traf2- and Nck complexed with a selective inhibitor, 9-hydroxy-4-phenyl-6*H*-pyrrolo[3,4-*c*]carbazole-1,3-dione (ligand id: 824) (PDB id: 2X7F) were downloaded in the .pdb format. The proteins were converted from pdb to pdbqt using the PyRX0.8.

Ligand preparation. The bound ligands were removed and redocked with the respective proteins to obtain the vina score to validate the docking tool and to obtain the interaction score. The ligand molecules were drawn using ACD ChemSketch and saved as a .mol file. The OPENBABEL program available inside

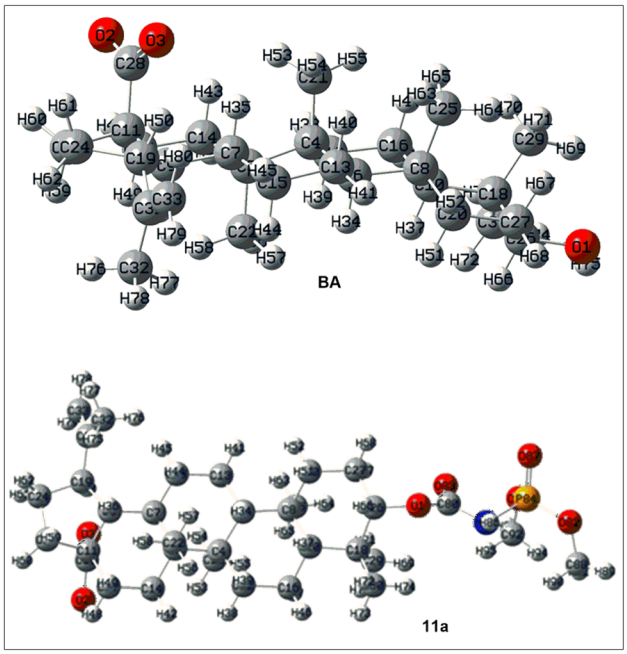

Fig. 2 Optimized structures of the representative compounds in their carboxylate form.

Table 1 IC_{50} values of BA and its derivatives against various cancer cell lines

Compound	Breast MCF-7	Lung A549	Colon HCT-116	Leukemia MOLT-4	Prostate PC-3	Pancreatic MiaPaca-2
1	22.86	24.74	12.23	44.30	15.55	16.72
8	19.13	18.15	11.15	>50	12.11	15.23
9a	19.24	>50	22.50	>50	>50	>50
9b	**13.00**	**12.59**	18.42	**18.02**	**12.00**	34.01
9c	>50	**9.21**	11.44	>50	**12.83**	29.00
9d	16.00	**9.98**	13.99	**8.35**	**12.36**	14.00
9e	**9.48**	**7.67**	**6.78**	**11.70**	**7.48**	**6.62**
9f	>50	**10.87**	**9.78**	>50	16.70	16.00
9g	>50	14.79	12.50	>50	15.36	45.00
10	**13.12**	**10.26**	**5.25**	**14.04**	**12.68**	**8.34**
11a	**7.15**	**8.00**	**3.13**	**13.88**	**8.00**	**6.96**
11b	**18.00**	**12.00**	**13.00**	**16.00**	**18.10**	**11.00**
12	>50	30.21	**6.82**	>50	13.12	>50
13	15.10	18.16	**8.25**	18.00	12.79	10.34
14a	>50	46.71	12.00	>50	41.14	23.00
14b	>50	>50	11.55	>50	42.16	32.00
Paclitaxel	<0.01	<0.01	0.09	0.05	0.03	0.07

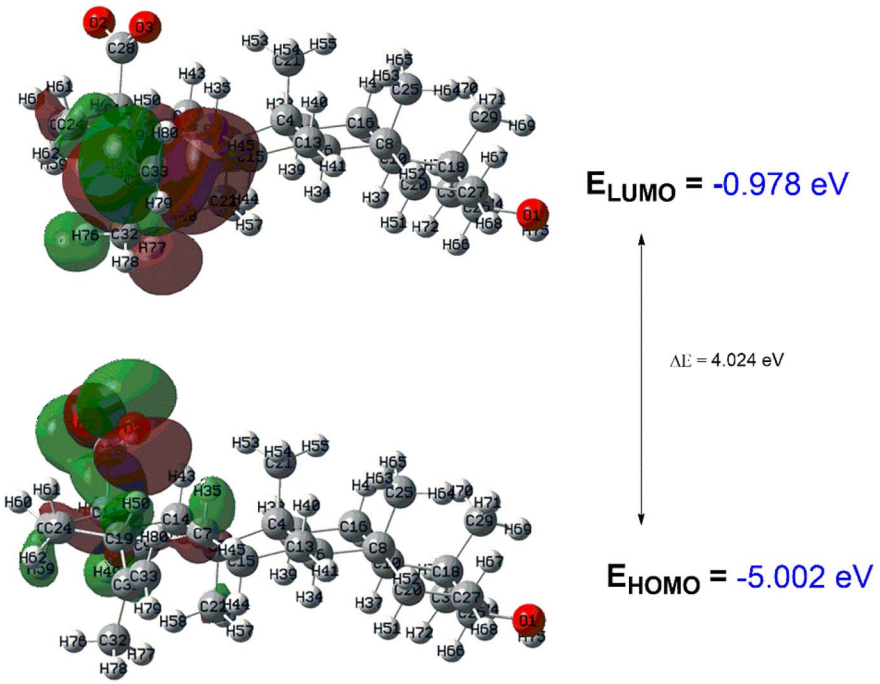

Fig. 3 FMO diagram of BA with the respective HOMO–LUMO gap.

the PyRX0.8 was used to convert all the molecules into PDB format, and universal force field (uff) was used for energy minimization with the number of runs kept to 2500.

Molecular docking. For docking studies, AutoDock vina program[17] was used. It is an efficient tool for prediction of protein–ligand binding. AutoGrid[17] was used to define docking area for proteins. The grid box size of 78 × 42 × 42 Å and centred at x, y, z coordinates of 8.78, 17.43, 26.21 for 1HOV, grid box size of 78, 71, 49 and grid center of 5.46, 0.09, 34.96 for 1UK0 and grid box size of 21, 0.31, 52 and grid center of 77.75, 57.64, 42.79 for 2X7F for all the ligands including reference to the target proteins. The AutoDock Vina exhaustiveness of 8 was applied using PyRx 0.8, a Graphical User Interface for docking

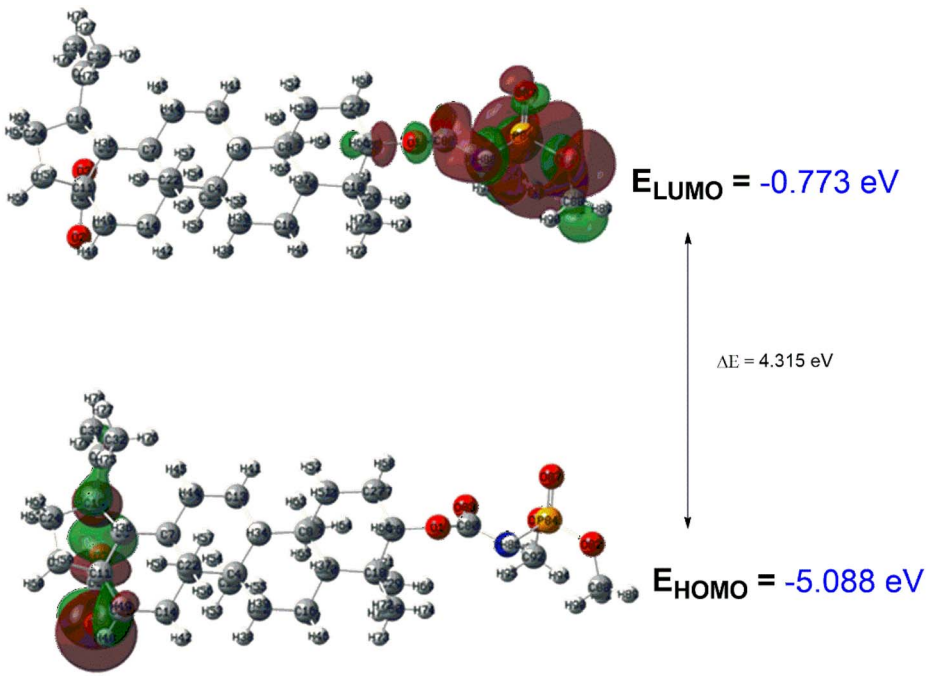

Fig. 4 FMO diagram of the **11a** with the respective HOMO–LUMO gap.

studies (Wolf, 2009). VinaLigGen was used to generate LigPlot for each conformation.[18–20]

Molecular dynamics simulation. MD simulations were performed on all three proteins by considering their APO form and the protein–ligand complex identified after the docking result using Desmond Maestro v11.3.[21] Initially, the protein preparation wizard was used to pre-process the protein and the system builder utility for preparing the system for simulation. The protein was then individually placed in an orthorhombic simulation box with a distance of 10 Å away from the edges. The system was solvated by pre-equilibrated simple point charge (SPC) water model and 0.15 M salt (NaCl) concentration was added along with Na^+ and Cl^- ions to neutralize the system. Prior to MD simulations, the model system was relaxed using the standard Desmond protocol. This a six-step relaxation protocol which includes an initial short simulation of 12 ps in NVT ensemble at $T = 10$ K with restraints on solute heavy atoms, a 12 ps simulation in NPT ensemble with $T = 10$ K and pressure (P) = 1 atm restraining the solute heavy atoms, a 12 ps simulation in NPT ensemble with restraints on nonhydrogen solute atoms, and a 24 ps simulation in NPT ensemble without restraints. The pressure and temperature conditions were stabilized with the isobaric and isothermal ensemble using the Martyna–Tobias–Klein barostat and Nosé–Hoover thermostat which are the default protocols of Desmond.

Finally, OPLS3 (ref. 22) force field was applied to the protein and ligand. System preparation included solvation, neutralization, minimization, and equilibration before a 100 ns NPT ensemble ($T = 300$ K and $P = 1$ atm) simulation and trajectory was recorded at intervals of 100 ps by generating approximately 1000 frames.

Result and discussion

Chemistry

The C-3-hydroxyl and C-20 double bond positions in BA are comparatively less explored than position C-28 with carboxylic acid. In this study we explored C-3 and C-20 positions and envisaged that introduction of nitrogen containing compounds (amine; oxime, phosphoramidate) could enhance the cytotoxic activity and even water solubility.[23,24] Additionally, BA derivatives containing an acyl moiety at C-3 position are known to display higher cytotoxicity.[23] To achieve this, we synthesised C-3 derived amine analogs with intact acyl group by treating compound **1** with chloroacetyl chloride in dry THF in presence of dry pyridine to synthesize intermediate **8** which was used as a starting material to synthesize target compounds. In order to keep the acyl group intact, compound **8** was subjected to react with different amines to afford desired products (**9a–g**) in excellent yields (Scheme 1).

The phosphoramidate moiety is known to improve the antitumor activity of the parent molecules.[25,26] Therefore, it was feasible to targeted C-3 and C-20 positions of betulinic acid. To synthesis C-3 derived phosphoramidate analogs, compound **2** with NaN_3 to furnish azide **10** with intact acetyl group. Compound **10** was treated with appropriate trialkyl phosphite in THF to produce the desired products **11a** and **11b** (Scheme 2).

Table 2 Reactive descriptors of the target compounds

Descriptor	BA	**11a**
E_{HOMO}	−0.978 eV	−0.773 eV
E_{LUMO}	−5.002 eV	−5.088
HOMO–LUMO gap	4.024 eV	4.315 eV
χ	−2.990	−2.930
σ	0.497	0.464
η	2.012	2.157
μ	22.72	29.77 D
Pi	2.990	2.930
ω	2.222	1.989

To synthesize phosphoramidate at C-20 position by exploiting the olefinic bond, compound **1** was treated with *N*-bromosuccinimide (NBS) to obtain **12** which when treated with NaN_3 afforded azide **13** that was finally treated with appropriate trialkyl phosphite to afford desired phosphoramidates **14a** and **14b** (Scheme 3). The structures of all the synthesized derivatives were confirmed using spectroscopic techniques.

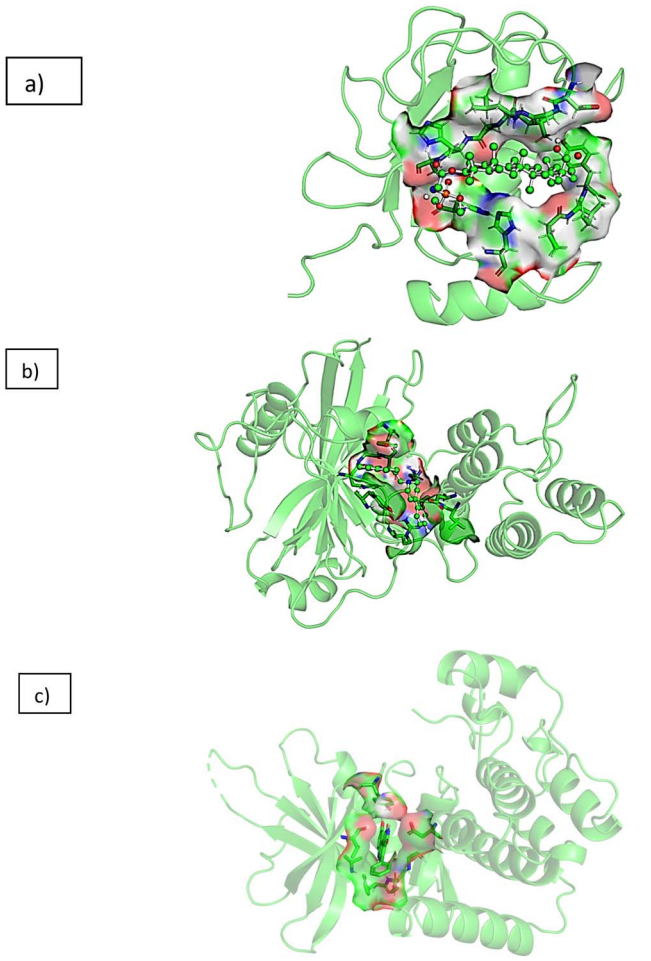

Fig. 5 3D interaction diagram of **11a** with (a) matrix metalloproteinase-2 (1HOV) (b) poly(ADP-ribose) polymerase (1UK0) (c) kinase domain of human Traf2- and Nck (2X7F).

Biology

All the derivatives including parent compound **1** were evaluated *in vitro* for anti-tumor activity on six different human cancer cell lines: breast cancer MCF-7, lung cancer A549, colon cancer HCT-116, leukaemia MOLT-4, prostate carcinoma cell PC-3 and pancreatic cancer cell Miapaca-2by MTT assay. The IC_{50} values are summarized in Table 1 and given as the average value of the triplicate analysis. As shown in Table 1, conversion of **1** to chloroacetyl chloride derivative **8**, slightly improved the activity. Among amine derivatives **9a–g** designed to evaluate the role played by amino moiety in influencing the anti-cancer activity **9b** was effective against MCF-7, A549, MOLT-4 and PC-3 cell lines with IC_{50} values 13.0, 12.59, 18.0 and 12.0 μM respectively and two to three times more active than **1** (BA). Compound **9d** was found active against A549, MOLT-4 and PC-3 cell lines with IC_{50} values between 9.98, 8.35 and 12.36 μM. **9e** was the most active compound among the amine derivatives having IC_{50}

Table 3 Vina score and hydrogen bonds for the ligand interacting with three proteins

Protein	Ligand	Vina score	Hydrogen bonds
1HOV	**1**	−6.8	HIS55|ARG53
	8	−7.5	—
	9a	−7.7	—
	9b	−8.1	—
	9c	−8.2	ALA86
	9d	−8.3	PRO75
	9e	−7.3	LEU128|HIS124|ALA86
	9f	−7.8	ALA86
	9g	−7.6	—
	10	−7	ARG38|ARG38
	11a	−7.2	ALA86|HIS85
	11b	−7.5	ALA86|HIS85
	12	−6.6	HIS55|ARG53
	13	−6.8	GLU30|ARG53
	14a	−7.3	—
	14b	−7.3	—
	i52	−6.5	ALA86| PHE87|HIS124|HIS120|HIS130
1UK0	**1**	−10	ASN207|GLU327
	8	−8.1	PRO281|LEU280|GLY283
	9a	−8.3	ASN207|SER203
	9b	−7.7	—
	9c	−10.5	SER203|ASP109|HIS201
	9d	−8	GLN46|SER213|ARG180
	9e	−9.9	SER203|HIS201|HIS201
	9f	−9.1	GLU102
	9g	−8.4	GLN98|ARG217
	10	−8.6	ASP105|SER322
	11a	−7.2	LEU117|SER121|GLU19
	11b	−9.8	HIS201|HIS201
	12	−8.9	—
	13	−7.5	GLY283|GLN335|TYR331|HIS285
	14a	−7.8	PRO189|PRO281|ASP332
	14b	−8.9	GLU327|HIS248
	FRM	−11.6	GLY202
2X7F	**1**	−6.9	GLY109|PHE107
	8	−6.8	GLY190
	9a	−6.8	LEU50|LEU50|GLN49
	9b	−7.1	—
	9c	−6.9	ASN164
	9d	−6.9	LEU50|LEU50
	9e	−6.6	THR84
	9f	−6.8	LEU50|LEU50
	9g	−6.8	LEU50|LEU50
	10	−6.9	LYS168|GLU106|THR84
	11a	−6.7	TYR86|PHE107|ARG80|ARG80
	11b	−6.2	GLU128|GLU127
	12	−6.8	TYR86
	13	−6.6	LEU50|LYS168|GLU106|LYS168|GLU106|THR84
	14a	−6.6	GLU163|TYR86|THR47
	14b	−6.3	LEU50|LYS168|TYR86
	824	−9.7	TYR36

values 9.48 (MCF-7), 7.67 (A549), 6.78 (HCT-116), 11.70 (MOLT-4), 7.48 (PC-3) and 6.62 (Miapaca-2) μM. Interestingly, both of these compounds (**9d** and **9e**) have a free hydroxyl group in the amino moiety. Compound **10** was effective against HCT-116 and Miapaca-2 cell lines, IC_{50} values 5.25 and 8.34 μM respectively. Among the phosphoramidate analogs, **11a** and **11b**, **11a** was two to four-fold more active than parent **1**, and found to be most active analog among all the synthesized derivatives, with IC_{50} values 7.15 (MCF-7), 8.00 (A549), 3.13 (HCT-116), 13.88 (MOLT-4), 8.00 (PC-3) and 6.96 (Miapaca-2) μM respectively on all the six cancer cell lines tested.

Compounds **12** and **13** were effective against HCT-116 cell line. In compounds **14a** and **14b**, the activity was significantly reduced compared to the parent **1** except for HCT-116 for which the activity was comparable to that of **1**. These results indicate that cytotoxicity profile of BA analogs may be susceptible to the size and the electrostatic sensitivity of the substituents present at C-20 position. In general, the above results demonstrated that

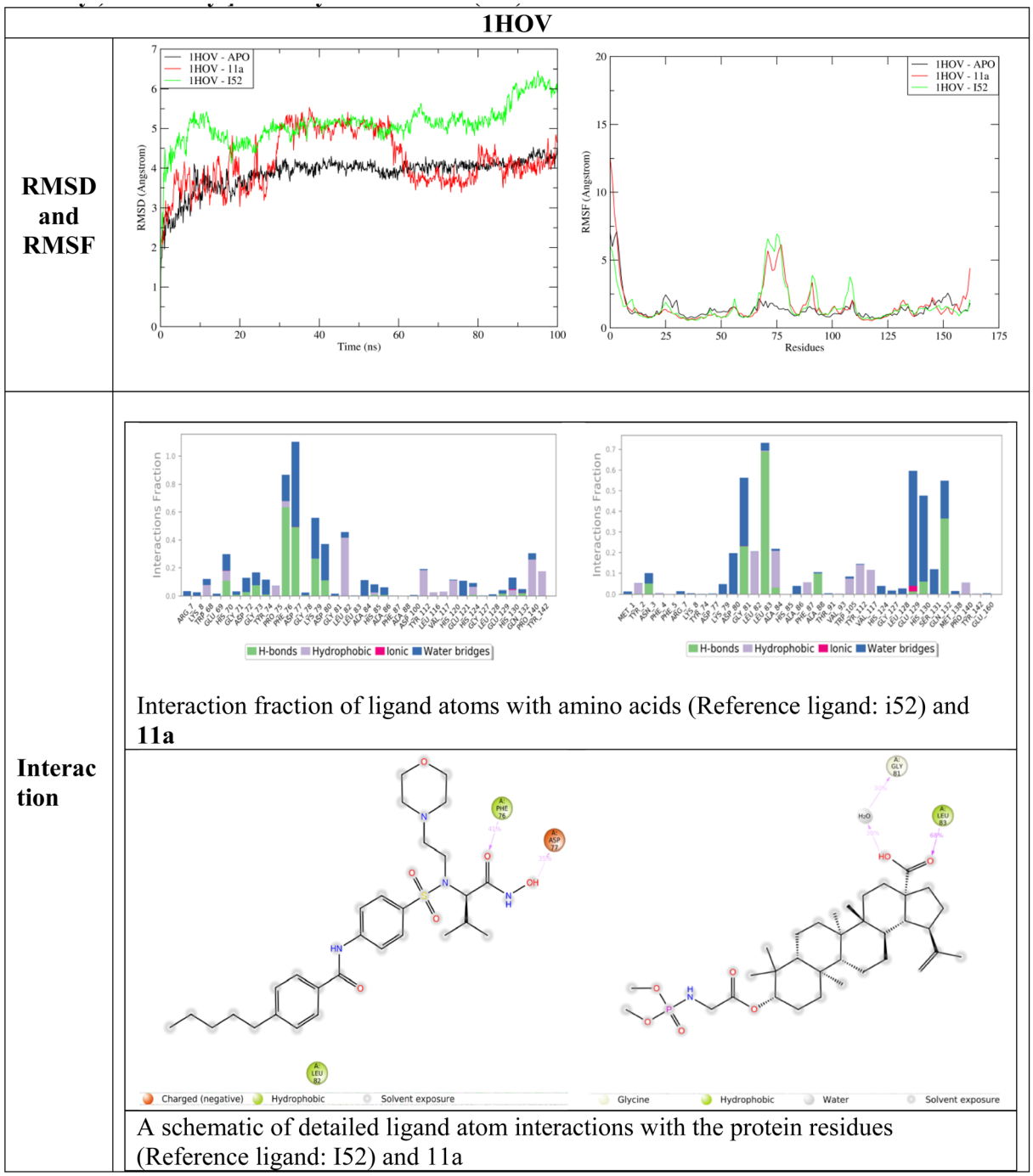

Fig. 6 RMSD, RMSF, interaction fraction and ligand–protein contacts between **11a** and reference ligand *N*-[[3-[4-[[(2*S*)-1-(hydroxyamino)-3-methyl-1-oxobutan-2-yl]sulfamoyl]phenyl]phenyl]methyl]-4-oxo-3*H*-quinazoline-2-carboxamide (I52) with 1HOV.

C-3 position was a favourable site to carry out structural modification to enhance the anti-tumor potential of BA. However, modification at C-20 resulted in the loss of activity indicated that C-20 position of BA was not a favourable site to derivatize to enhance cytotoxicity against cancer cell lines.

DFT-based global reactive descriptors

Geometry optimization is the first step of configuration/conformational analysis to arrive at a minimal energy state of a molecular system, provided no negative frequency is obtained in the calculation. Both molecular structures in their anionic forms were optimized at the relevant level of theory given in the computational methodology. Different optimization parameters, including bond lengths, bond angles, and dihedral angles of the parent compound, betulinic acid, and the potent derivative **11a** in their carboxylate form, can be visualized as given in Fig. 2. The frontier orbitals of both structures are shown in Fig. 3 and 4, respectively, for BA and **11a**.[27–30] The frontier molecular orbitals (FMO) play an important role in describing the reactivity of a molecule in association with global reactive descriptors given in Table 2. From the calculated reactive descriptors, it is clear that BA has more kinetic stability than **11a** due to a higher HOMO–LUMO gap, and the latter by global softness, global hardness, and dipole moment. These factors

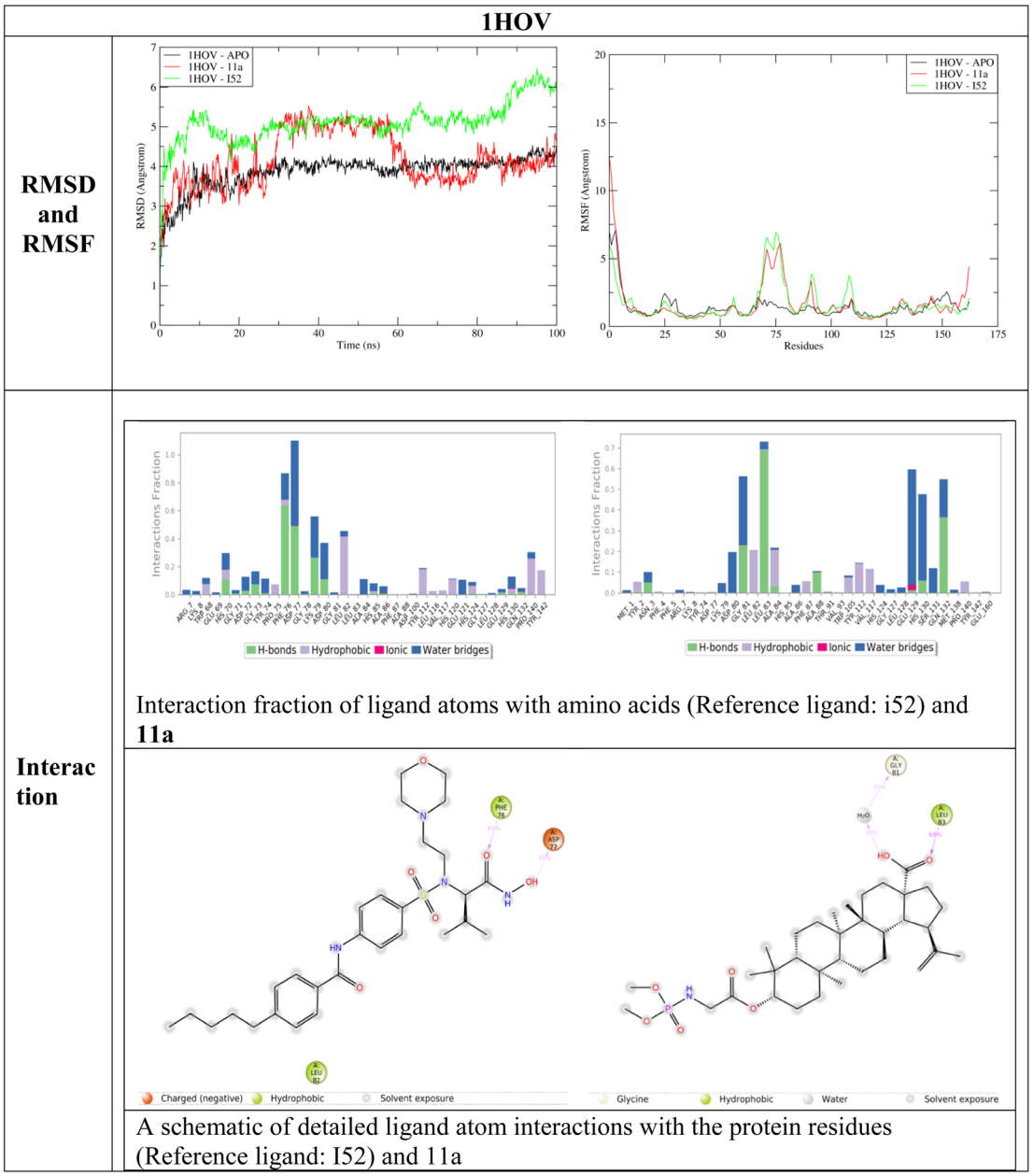

Fig. 7 RMSD, RMSF, Interaction fraction and ligand–protein contacts between **11a** and reference 2-{3-[4-(4-fluorophenyl)-3,6-dihydro-1(2*H*)-pyridinyl]propyl}-8-methyl-4(3*H*)-quinazolinone (RFM) with 1UK0.

are hence responsible for the fascinating bioactivity exhibited by **11a**.

Molecular docking

From the *in vitro* studies, compound **11a** was found to be the lead compound with maximum activity against colon cancer cell line HCT-116 (IC_{50} value 3.13 μM), hence taken for molecular docking studies to get insights into the molecular mode of action against colon cancer. As mentioned in our recent publication three targets involved in pathophysiology of colon cancer including matrix metalloproteinase-2 (PDB ID: 1HOV), poly[ADP-ribose] polymerase-1 (PDB ID: 1UK0) and TRAF2 (PDB ID: 2X7F) were chosen to elucidate the mechanism of action against colon cancer.[31] Fig. 5 represents the 3D interactions of **11a** with all the three proteins mentioned above. Table 3 represent the data obtained from Molecular Docking analysis of all the synthesized compounds **1**, **8**, **9a–g**, **10**, **11a** and **11b**, **12**, **13**, **14a** and **14b** along with the parent molecule 1. Post docking analysis like hydrogen bond and hydrophobic interactions between each conformation of ligand with protein was performed using VinaLigGenand. The ligands which showed better vina score along with interaction were further considered for dynamics simulation. It was observed that the reference ligands I52 (PDB 1HOV) formed five hydrogen bonds with Ala86, Phe87, His124, His120 and His130 with vina score of −6.5, co-crystallised inhibitor FRM (PDB 1UK0) forms one hydrogen bond with Gly202 with vina score of −11.6 and co-crystallised

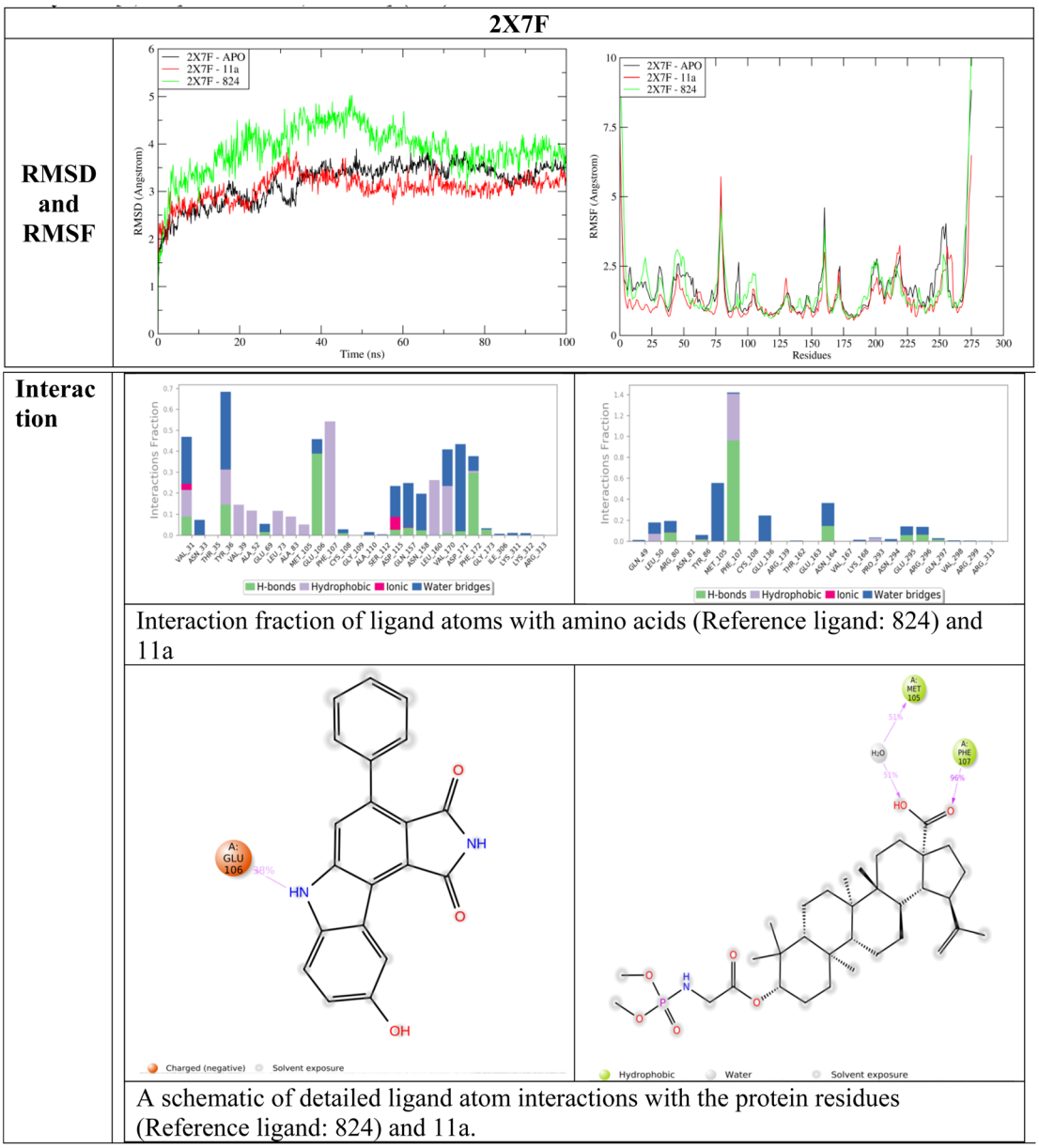

Fig. 8 RMSD, RMSF, interaction fraction and ligand–protein contacts between **11a** and reference 9-hydroxy-4-phenylpyrrolo[3,4-*c*]carbazole-1,3(2*H*,6*H*)-dione[9-hydroxy-4-phenyl-6*H*-pyrrolo[3,4-*c*]carbazole-1,3-dione] (824) with 2X7F.

inhibitor 824 (PDB 2X7F) forms one hydrogen bond with Tyr36 with the vina score of −9.7. All the interactions matched with the interactions available at the PdbSum to validate the docking tool and to consider the vina score as reference.[32–34]

Based on the vina score, interactions and the *in vitro* studies the ligand **11a** exhibited the vina score of −7.2 with 1HOV protein. In the case of 1UK0, it formed three hydrogen bonds with Leu117, Ser121, Glu19, yielding a vina score of −7.2. Ligand displayed the vina score of −6.7 by forming four hydrogen bonds with Tyr86, Phe107 and Arg80 for 2X7F. These complexes were subsequently chosen for dynamics simulation.

Molecular dynamics simulation

Molecular dynamics simulation studies provide a detailed account of binding interactions and interaction stability related to protein and ligand. The two terms RMSD provide details about structure deviation and RMSF detailed about the protein fluctuations due to ligand interactions.[27] Fig. 6–8 represent the RMSD, RMSF, interaction fraction and ligand protein contacts between **11a** and three proteins 1HOV, 1UK0 and 2X7F respectively.

During the interaction study with 1HOV, the RMSD plot indicates that the ligand-bound form shows structural deviations throughout the simulation time of 100 ns. The unbound form of the protein maintains stability. The deviation in the complex form (both reference ligand I52 and **11a**) of the protein due to fluctuations in amino acid position 60–85. There is a significant secondary structural change around the residues 82–85. In the APO form, beta-sheet is formed while in the complex the beta sheet is completely lost throughout the simulation time of 100 ns bringing more deviation to the protein complex. Interaction analysis of reference ligand I52 shows hydrophobic interaction with Phe76, and Leu82, hydrogen bond with Asp77. Ligand **11a** formed hydrophobic interaction with fraction values near 0.7 with Leu83 and formed water bridge with Gly81. These residues constitute the binding site of the protein as observed in PDBSum (1HOV – Sc-74020 complex). Overall, ligand **11a** exhibits deviation around 30 ns and 60 ns and stability after the simulation time of 60 ns.

The RMSD analysis of **11a** with 1UK0 indicates that binding of ligand **11a** reduces overall deviation compared to the APO form when compared with reference ligand FRM. Notably, there is a significant reduction in fluctuation around positions 50–60, 110–130 and 150–260 supporting in deviation reduction. The reference ligand formed hydrogen bond with Gly202 and Asn207. Hydrophobic interaction with Leu108, His201, Tyr235, Tyr246. Ligand **11a** formed a weak interaction between ligand and multiple residues Lys13, Asp17, Leu117, Gly119 and Asn132 was observed. Since interaction fraction less than 0.4, residues were not observed between the ligand–protein contact analysis.

From the RMSD analysis, both reference and **11a** demonstrated stability with 2X7F. However, compared to reference 824, the overall deviation slightly decreases in the **11a** complex after 35 ns of simulation time. Reduction in fluctuation is observed in the initial positions, 220 to 260, contributing to a significant deviation compared to the APO form. A hydrogen bond with Phe107 was observed for both the ligands and water bridge formation with Met105 for **11a**. The protein–ligand complex shows a stable interaction is the active site.

Conclusion

In this paper, different synthetic strategies were used to exploit C-3 and C-20 positions of betulinic acid to design and synthesized novel derivatives to evaluate their effect on anticancer activity. All the analogs were tested *in vitro* for anti-tumor activity on six different human cancer cell lines including breast cancer MCF-7, lung cancer A549, colon cancer HCT-116, leukaemia MOLT-4, prostate carcinoma PC-3 and pancreatic cancer Miapaca-2 by MTT assay. Many derivatives displayed better cytotoxicity profile than the parent compound. More significantly compounds **9b**, **9e**, **10** and **11a** were found to have promising activity profile than BA. Compound **11a** was found as the most potent and lead compound, with maximum activity against colon cancer HCT-116 cell line (IC_{50} values 3.13 μM). DFT calculation also supports the observed data followed by the molecular docking and dynamic studies of compound **11a** showing more stable interactions with protein 2X7F. Compound **11a** exhibited the potential to be developed as potent anticancer agent against colon cancer and should be further explored for *in vitro* and *in vivo* mechanism of action studies against colon cancer.

Data availability

The associated data with this article can be found in ESI.†

Conflicts of interest

There is no conflict of interest associated with this article.

Author contributions

Nisar A. Dangroo: conceptualization, data interpretation, writing – original draft, Ziad Moussa: funding acquisition/review drafting/data interpretation, Mustafa S. Alluhaibi: *in silico*/software, Abdulrahman A. Alsimaree: *in silico*/software, Mohammed B. Hawsawi: docking, Reem I. Alsantali: methodology investigation, Jasvinder Singh: methodology, investigation, bioassays, Nidhi Gupta: manuscript writing, editing and MD, Basavarajaiah S. M.: software Md simulations, molecular docking, Prashantha Karunakar: molecular docking and MD study, J. M. Mir: Gaussian based DFT calculations, Manzoor A. Rather: formal analysis and characterization, and Saleh A. Ahmed: supervision, review, editing and fund acquisition.

Acknowledgements

The authors extend their appreciation to Taif university, Saudi Arabia, for supporting this work through project number (TU-DSPP-2024-86). Ziad Moussa is grateful to the United Arab Emirates University (UAEU) and to the Research Office for supporting the research developed in his laboratory and

reported herein (UPAR grant code G00004605). NAD sincerely thanks the Department of Science and Technology-Science and Engineering Research Board (DST-SERB) New Delhi, India for providing fellowship under File No. PDF/20l7/002716CS.

References

1 **https://www.who.int/news-room/fact-sheets/detail/cancer**, accessed on 18.06.2024.
2 **https://www.who.int/news-room/fact-sheets/detail/colorectal-cancer**, accessed on 18.06.2024.
3 **https://www.cancer.gov/types/colorectal/patient/colon-treatment-pdq**, accessed on 18.06.2024.
4 D. J. Newman and G. M. Cragg, *J. Nat. Prod.*, 2020, **83**, 770–803.
5 Y. Ren and A. D. Kinghorn, *Planta Med.*, 2019, **85**, 802–814.
6 X. Zhang, J. Hu and Y. Chen, *Mol. Med. Rep.*, 2016, **14**, 4489–4495.
7 Y. Zhong, N. Liang and M.-S. CHENG, *Chin. J. Nat. Med.*, 2021, **19**, 641–647.
8 R. Csuk, *Expert Opin. Ther. Pat.*, 2014, **24**, 913–923.
9 Y. Zhang, S. Ye, Y. Wang, C. Wang, Y. Zhu, Y. Wu, Y. Zhang, H. Zhang and Z. Miao, *Bioorg. Med. Chem.*, 2022, **59**, 116672.
10 G. Liebscher, K. Vanchangiri, T. Mueller, K. Feige, J.-M. Cavalleri and R. Paschke, *Chem.-Biol. Interact.*, 2016, **246**, 20–29.
11 N. Gupta, S. K. Rath, J. Singh, A. Qayum, S. Singh and P. L. Sangwan, *Eur. J. Med. Chem.*, 2017, **135**, 517–530.
12 N. A. Dangroo, J. Singh, S. K. Rath, N. Gupta, A. Qayum, S. Singh and P. L. Sangwan, *Steroids*, 2017, **123**, 1–12.
13 I. Khan, S. K. Guru, S. K. Rath, P. K. Chinthakindi, B. Singh, S. Koul, S. Bhushan and P. L. Sangwan, *Eur. J. Med. Chem.*, 2016, **108**, 104–116.
14 C. J. Brabec and N. S. Sarici, *Adv. Funct. Mater.*, 2001, **11**, 15–26.
15 W. J. Hehre, R. Ditchfield and J. A. Pople, *J. Chem. Phys.*, 1972, **56**, 2257–2261.
16 M. J. Frisch, G. W. Trucks, H. B. Schlegel, G. E. Scuseria, M. A. Robb, J. R. Cheeseman, G. Scalmani, V. Barone, B. Mennucci, G. A. Petersson, H. Nakatsuji, M. Caricato, X. Li, H. P. Hratchian, A. F. Izmaylov, J. Bloino, G. Zheng, J. L. Sonnenberg, M. Hada, M. Ehara, K. Toyota, R. Fukuda, J. Hasegawa, M. Ishida, T. Nakajima, Y. Honda, O. Kitao, H. Nakai, T. Vreven, J. A. Montgomery Jr, J. E. Peralta, F. Ogliaro, M. Bearpark, J. J. Heyd, E. Brothers, K. N. Kudin, V. N. Staroverov, T. Keith, R. Kobayashi, J. Normand, K. Raghavachari, A. Rendell, J. C. Burant, S. S. Iyengar, J. Tomasi, M. Cossi, N. Rega, J. M. Millam, M. Klene, J. E. Knox, J. B. Cross, V. Bakken, C. Adamo, J. Jaramillo, R. Gomperts, R. E. Stratmann, O. Yazyev, A. J. Austin, R. Cammi, C. Pomelli, J. W. Ochterski, R. L. Martin, K. Morokuma, V. G. Zakrzewski, G. A. Voth, P. Salvador, J. J. Dannenberg, S. Dapprich, A. D. Daniels, O. Farkas, J. B. Foresman, J. V. Ortiz, J. Cioslowski, and D. J. Fox, *GAUSSIAN 09 (Revision C.01)*, Gaussian, Inc., Wallingford CT, 2010.
17 O. Trott and A. J. Olson, *J. Comput. Chem.*, 2010, **31**, 455–461.
18 G. M. Morris, D. S. Goodsell, R. S. Halliday, R. Huey, W. E. Hart, R. K. Belew and A. J. Olson, *J. Comput. Chem.*, 1998, **19**, 1639–1662.
19 S. Thandivel, P. Rajan, T. Gunasekar, A. Arjunan, S. Khute, S. R. Kareti and S. Paranthaman, *Heliyon*, 2024, **10**, e27880.
20 A. C. Wallace, R. A. Laskowski and J. M. Thornton, *Protein Eng., Des. Sel.*, 1995, **8**, 127–134.
21 S. Dallakyan and A. J. Olson, in *Chemical Biology*, ed. J. E. Hempel, C. H. Williams and C. C. Hong, Springer New York, New York, NY, 2015, vol. 1263, pp. 243–250.
22 K. J. Bowers, F. D. Sacerdoti, J. K. Salmon, Y. Shan, D. E. Shaw, E. Chow, H. Xu, R. O. Dror, M. P. Eastwood, B. A. Gregersen, J. L. Klepeis, I. Kolossvary and M. A. Moraes, in *Proceedings of the 2006 ACM/IEEE Conference on Supercomputing SC '06*, ACM Press, Tampa, Florida, 2006, p. 84.
23 J. Wiemann, L. Heller, V. Perl, R. Kluge, D. Ströhl and R. Csuk, *Eur. J. Med. Chem.*, 2015, **106**, 194–210.
24 M. Willmann, V. Wacheck, J. Buckley, K. Nagy, J. Thalhammer, R. Paschke, T. Triche, B. Jansen and E. Selzer, *Eur. J. Clin. Invest.*, 2009, **39**, 384–394.
25 F. M. Oliveira, L. C. Barbosa and F. M. Ismail, *RSC Adv.*, 2014, **4**, 18998–19012.
26 C. R. Wagner, V. V. Iyer and E. J. McIntee, *Med. Res. Rev.*, 2000, **20**, 417–451.
27 P. J. Stephens, D. M. McCann, F. J. Devlin and A. B. Smith, *J. Nat. Prod.*, 2006, **69**, 1055–1064.
28 T. Erdogan, *J. Mol. Struct.*, 2021, **1242**, 130733.
29 D. F. Tegegn, H. Z. Belachew and A. O. Salau, *Sci. Rep.*, 2024, **14**, 8146.
30 C. F. Matta, *J. Comput. Chem.*, 2014, **35**, 1165–1198.
31 C.-H. Lai, C.-C. Chang, Y.-L. Weng and T.-H. Chuang, *Molecules*, 2018, **23**, 3170.
32 E. O. Akintemi, K. K. Govender and T. Singh, *Comput. Theor. Chem.*, 2022, **1210**, 113658.
33 N. Gupta, G. Singh, A. Qayum, M. Ovais Dar, S. Singh, M. Katoch and P. L. Sangwan, *ChemistrySelect*, 2024, **9**, e202400637.
34 S. M. Basavarajaiah, J. Badiger, N. G. Yernale, N. Gupta, P. Karunakar, B. T. Sridhar, M. Javeed, K. S. Kiran and B. Rakesh, *Bioorg. Chem.*, 2023, **137**, 106598.